Appendix A. Flexible Wall Adjust Mechanism (FWAM) Design

Table A-1 FWAM Parts List

Part Name	Quantity	McMaster-Carr Catalog Number	Material	Description
Block	2	See Drawing	T6 Aluminum	Custom machined block fabricated by VT machine shop.
Male Hinge	2	See Drawing	T6 Aluminum	Hinge componet to join Block to Female Hinge. Fabricated by VT machine shop.
Female Hinge	2	See Drawing	T6 Aluminum	Hinge component to bolt FWAM assembly to the flexible wall.
Hinge Pin	2		Aluminum	3/16" diameter 1" long pin to join Female and Male Hinge components. Purchased at Mish-Mish art supply store.
3/8" ID Set-Screw Shaft Collar	2	6432K14	Steel	Slides on Rod and fastened by set-screw. Resides in Block slot.
Coarse-Pitch Spur Gear	2	6325K88	Steel	24 Pitch, 1" Pitch Diameter, 3/8" ID. Install set-screw and fasten to Rod. Meshes with Rack on Block.
Coarse-Pitch Rack	2	6295K12	Steel	24 Pitch Shipped 24" long. Cut to length of block.
Rod	1	5947K48	1045 Steel	3/8" OD, 36" Long. Machine flats wherever set screw will fasten (optional).
Knurled-Rim Clamping Knob (Unthreaded)	1	6121K17	Steel	Handle to turn Rod. Install set-screw and fasten to Rod end.

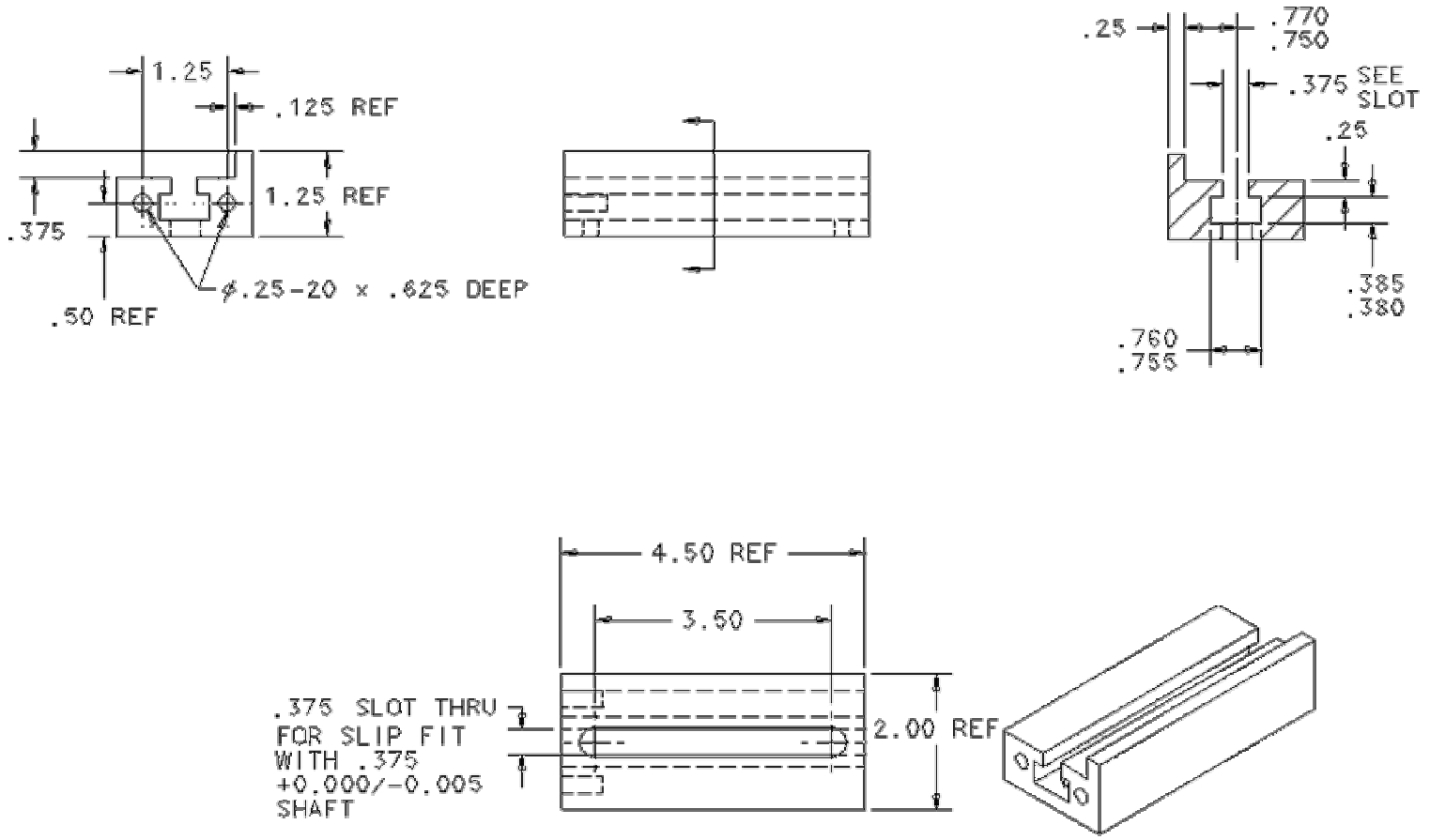

Figure A-1 T6 Aluminum Block Schematic.

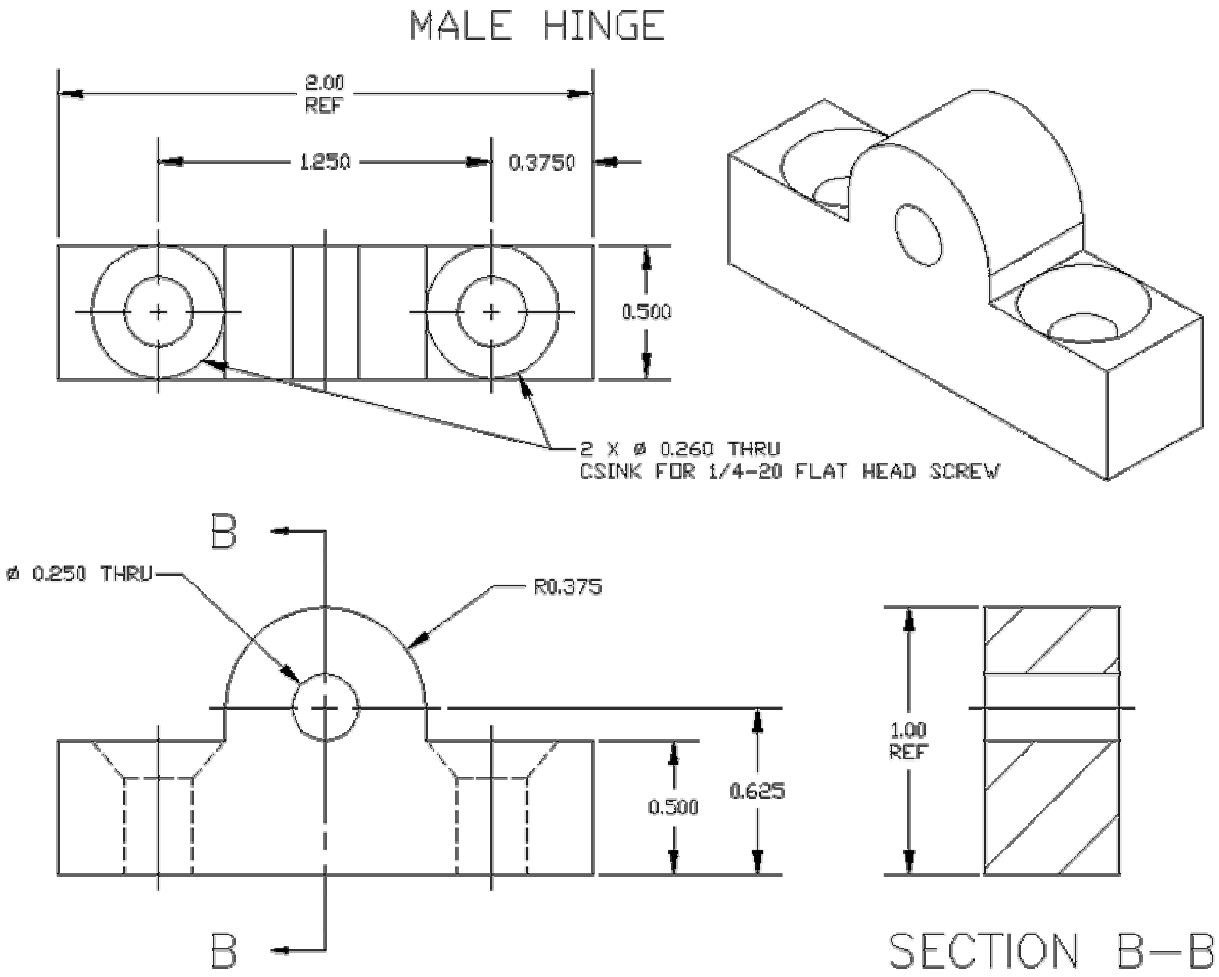

Figure A-2 T6 Aluminum Male Hinge Schematic.

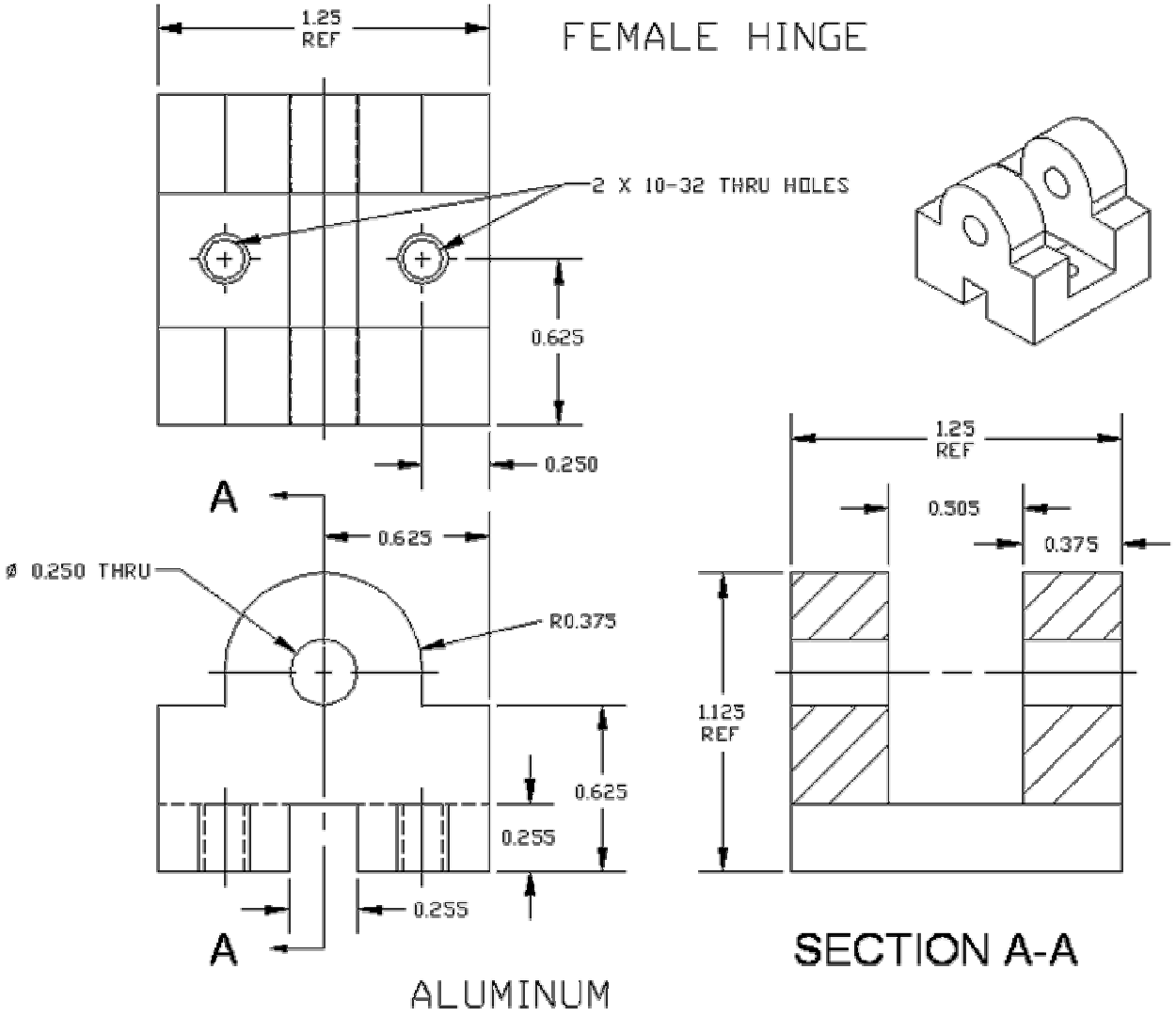

Figure A-3 T6 Aluminum Female Hinge Schematic.

Appendix B. Blade Profile Coordinates

The coordinates of the basic blade outline used throughout this study are tabulated below, first with the pressure side points and second with the suction side points. The stagnation point has been assigned as the origin.

Pressure Side	
y (cm)	**x (cm)**
-40.0829	34.9930
-40.2677	34.9711
-40.4413	34.9046
-40.5932	34.7973
-40.7138	34.6556
-40.7959	34.4889
-40.8342	34.3066
-40.8265	34.1210
-40.7732	33.9427
-40.6775	33.7833
-40.5455	33.6522
-40.3853	33.5577
-40.2256	33.4885
-40.0543	33.4145
-39.8591	33.3334
-39.6409	33.2450
-39.4008	33.1475
-39.1395	33.0408
-38.8575	32.9250
-38.5552	32.8006
-38.2331	32.6683
-37.8916	32.5278
-37.5313	32.3797
-37.1530	32.2230
-36.7573	32.0575
-36.3446	31.8844
-35.9152	31.7039
-35.4697	31.5159
-35.0089	31.3202
-34.5329	31.1178
-34.0426	30.9078
-33.5386	30.6902
-33.0218	30.4649
-32.4924	30.2322
-31.9509	29.9924
-31.3977	29.7460
-30.8333	29.4932
-30.2585	29.2337
-29.6738	28.9674

Pressure Side (cont'd)	
y (cm)	**x (cm)**
-29.0801	28.6941
-28.4779	28.4137
-27.8677	28.1264
-27.2501	27.8324
-26.6255	27.5320
-25.9948	27.2249
-25.3586	26.9107
-24.7178	26.5893
-24.0729	26.2606
-23.4244	25.9251
-22.7727	25.5832
-22.1189	25.2341
-21.4642	24.8767
-20.8089	24.5117
-20.1533	24.1399
-19.4985	23.7604
-18.8458	23.3722
-18.1959	22.9756
-17.5492	22.5710
-16.9066	22.1582
-16.2692	21.7367
-15.6380	21.3062
-15.0140	20.8665
-14.3982	20.4175
-13.7914	19.9594
-13.1949	19.4918
-12.6098	19.0144
-12.0374	18.5270
-11.4790	18.0297
-10.9354	17.5226
-10.4075	17.0065
-9.8955	16.4823
-9.4006	15.9502
-8.9245	15.4101
-8.4682	14.8624
-8.0323	14.3081
-7.6172	13.7485
-7.2231	13.1845
-6.8500	12.6175

Pressure Side (cont'd)	
y (cm)	**x (cm)**
-6.4986	12.0485
-6.1679	11.4791
-5.8576	10.9110
-5.5671	10.3453
-5.2971	9.7829
-5.0468	9.2251
-4.8149	8.6737
-4.6003	8.1301
-4.4025	7.5953
-4.2205	7.0703
-4.0544	6.5563
-3.9023	6.0544
-3.7630	5.5659
-3.6350	5.0917
-3.5176	4.6329
-3.4116	4.1897
-3.3180	3.7628
-3.2339	3.3532
-3.1534	2.9630
-3.0693	2.5942
-2.9684	2.2326
-2.8431	1.8784
-2.6907	1.5353
-2.5097	1.2063
-2.2991	0.8950
-2.0546	0.6102
-1.7733	0.3613
-1.4584	0.1571
-1.1119	0.0144
-0.7446	-0.0605
-0.3697	-0.0651
0.0000	0.0000

Suction Side	
y (cm)	**x (cm)**
0.3545	0.1241
0.6889	0.2953
1.0010	0.5047
1.2897	0.7450
1.5561	1.0098
1.8011	1.2945
2.0261	1.5953
2.2324	1.9092
2.4217	2.2336
2.5863	2.5495
2.7460	2.8927
2.8984	3.2605
3.0426	3.6520
3.1764	4.0666
3.2977	4.5038
3.4022	4.9633
3.4870	5.4443
3.5498	5.9456
3.5879	6.4655
3.5988	7.0025
3.5805	7.5546
3.5318	8.1198
3.4510	8.6957
3.3379	9.2804
3.1925	9.8718
3.0145	10.4677
2.8030	11.0659
2.5582	11.6643
2.2815	12.2616
1.9745	12.8564
1.6387	13.4476
1.2741	14.0337
0.8818	14.6136
0.4640	15.1866
0.0214	15.7523
-0.4437	16.3105
-0.9302	16.8607
-1.4377	17.4019
-1.9650	17.9336

Suction Side (cont)	
y (cm)	**x (cm)**
-2.5109	18.4557
-3.0742	18.9681
-3.6536	19.4711
-4.2479	19.9643
-4.8563	20.4474
-5.4787	20.9196
-6.1139	21.3810
-6.7604	21.8320
-7.4173	22.2730
-8.0836	22.7041
-8.7584	23.1250
-9.4420	23.5346
-10.1335	23.9328
-10.8315	24.3204
-11.5350	24.6985
-12.2429	25.0671
-12.9548	25.4262
-13.6698	25.7762
-14.3871	26.1173
-15.1061	26.4497
-15.8259	26.7736
-16.5460	27.0893
-17.2655	27.3972
-17.9839	27.6973
-18.7005	27.9898
-19.4148	28.2749
-20.1260	28.5528
-20.8334	28.8241
-21.5363	29.0895
-22.2340	29.3493
-22.9262	29.6028
-23.6125	29.8499
-24.2924	30.0907
-24.9650	30.3259
-25.6298	30.5554
-26.2865	30.7795
-26.9345	30.9977
-27.5733	31.2101
-28.2022	31.4174

Suction Side (cont)	
y (cm)	**x (cm)**
-28.8209	31.6195
-29.4288	31.8161
-30.0255	32.0072
-30.6106	32.1922
-31.1833	32.3727
-31.7432	32.5479
-32.2898	32.7177
-32.8229	32.8820
-33.3419	33.0405
-33.8461	33.1941
-34.3351	33.3422
-34.8084	33.4858
-35.2656	33.6236
-35.7065	33.7549
-36.1306	33.8799
-36.5372	33.9997
-36.9258	34.1140
-37.2958	34.2228
-37.6470	34.3261
-37.9788	34.4234
-38.2910	34.5139
-38.5830	34.5986
-38.8543	34.6772
-39.1044	34.7495
-39.3329	34.8156
-39.5398	34.8738
-39.7249	34.9226
-39.8986	34.9683
-40.0829	34.9930

Appendix C. Material Properties of Alumina.

Table C-1 Material Properties of Alumina

Property	Units	Value
Density	kg/m^3	2803
Shrinkage (as cast)	%	NIL
Shrinkage (at 1000°F)	%	1.25
Comp. Strength	kPa	17237
Modules of Rupture	kPa	6895
Thermal Expansion	x 10^{-6}/°C	7.2
Thermal Conductivity	W / m K	1.44
Dielectric Strength	V / mm	6890
Color		White

Resbond was used to repair cracks in the alumina material.

Table C-2 Material Properties of Resbond

Property	Units	Value
Max Use Temperature	°C	1649
Continuous Service Temp.	°C	1288
Density	kg/m^3	1602-1922
Compressive Strength	kPa	24132
Elongation	%	5
Specific Heat	J / kg K	1046
Dielectric Constant	@ 10^8 cps	3
Volume Resistivity	ohm-cm	109
Dielectric Strength	V/mm	5709
Thermal Conductivity	W / m K	0.87
Shrinkage	%	2

Appendix D. Static Pressure Tap Locations

This Appendix lists the locations of midspan and shroud pressure taps that were used in the wind tunnel.

Table D-1 Midspan Pressure Tap Locations

	Designation Number	Location from Stagnation (S/Smax)
Pressure Side	1	-0.699
	2	-0.505
	3	-0.266
	4	-0.115
	5	-0.062
	6	-0.035
	7	-0.018
Stagnation	8	0.000
Suction Side	9	0.016
	10	0.031
	11	0.055
	12	0.070
	13	0.188
	14	0.305
	15	0.485
	16	0.633

Table D-2 Shroud Tap Locations

Index	x (in)	y (in)
1	-0.040	0.515
2	-0.038	0.385
3	-0.035	0.249
4*	-0.004	0.384
5	-0.004	0.461
6	-0.002	0.577
7	0.000	0.304
8	0.003	0.358
9	0.004	0.373
10	0.011	0.387
11	0.015	0.407
12	0.023	0.201
13	0.023	0.357
14	0.031	0.400
15	0.033	0.345
16	0.036	0.415
17	0.040	0.377
18	0.049	0.405
19	0.050	0.523
20	0.052	0.349
21	0.058	0.422
22	0.061	0.365
23	0.065	0.391
24	0.067	0.334
25	0.071	0.412
26	0.079	0.374
27	0.080	0.300
28	0.083	0.420
29	0.087	0.326
30	0.087	0.338
31	0.090	0.407
32	0.101	0.352
33	0.104	0.317
34	0.107	0.475
35	0.111	0.380
36	0.111	0.414
37	0.115	0.398
38	0.120	0.290
39	0.121	0.102
40	0.121	0.218
41	0.123	0.323
42	0.124	0.355
43	0.135	0.300
44	0.140	0.397
45	0.146	0.379
46	0.150	0.285
47	0.151	0.249
48	0.151	0.300
49	0.158	0.327
50	0.163	0.277
51	0.170	0.424
52	0.175	0.230
53	0.175	0.373
54	0.177	0.276
55	0.178	0.128
56	0.180	0.346
57	0.182	0.303
58	0.184	0.253
59	0.186	0.233
60	0.195	0.258
61	0.199	0.235
62	0.202	0.039
63	0.204	0.340
64	0.209	0.318
65	0.210	0.175
66	0.211	0.234
67	0.211	0.273
68	0.214	0.210
69	0.214	0.221
70	0.216	0.365
71	0.220	0.150
72	0.229	0.215
73	0.230	0.188
74	0.232	0.174
75	0.232	0.277
76	0.232	0.301
77	0.236	0.238
78	0.240	0.194
79	0.242	0.159
80	0.243	0.208
81	0.251	0.265
82	0.252	0.326
83	0.254	0.237
84	0.257	0.055
85	0.261	0.111
86	0.266	0.141
87	0.268	0.111
88	0.273	-0.042
89	0.278	0.081
90	0.280	0.210
91	0.285	0.098
92	0.287	0.164
93	0.291	0.060
94	0.292	0.088
95	0.296	0.092
96	0.297	0.267
97	0.309	0.132
98	0.311	0.094
99	0.316	0.198
100	0.317	0.037
101	0.318	-0.004
102	0.326	-0.070
103	0.331	0.064
104	0.332	0.025
105	0.340	0.125
106	0.343	-0.021
107	0.350	-0.002
108	0.361	0.178
109	0.371	0.028
110	0.385	-0.068
111	0.403	0.082
112	0.435	-0.038
Additional Points 9-3-02		
113	0.136	0.311
114	0.164	0.288
115	0.221	0.224
116	0.253	0.169
117	0.255	0.138
118	0.280	0.120
119	0.306	0.059
120	0.308	0.026
121	0.325	0.095
122	0.335	0.154

*Stagnation Location

Appendix E. Components for Infrared Camera Window Setup.

This appendix contains schematics for the aluminum IR window frame, the lexan lid, and the lexan shroud that are described in Chapter 3.

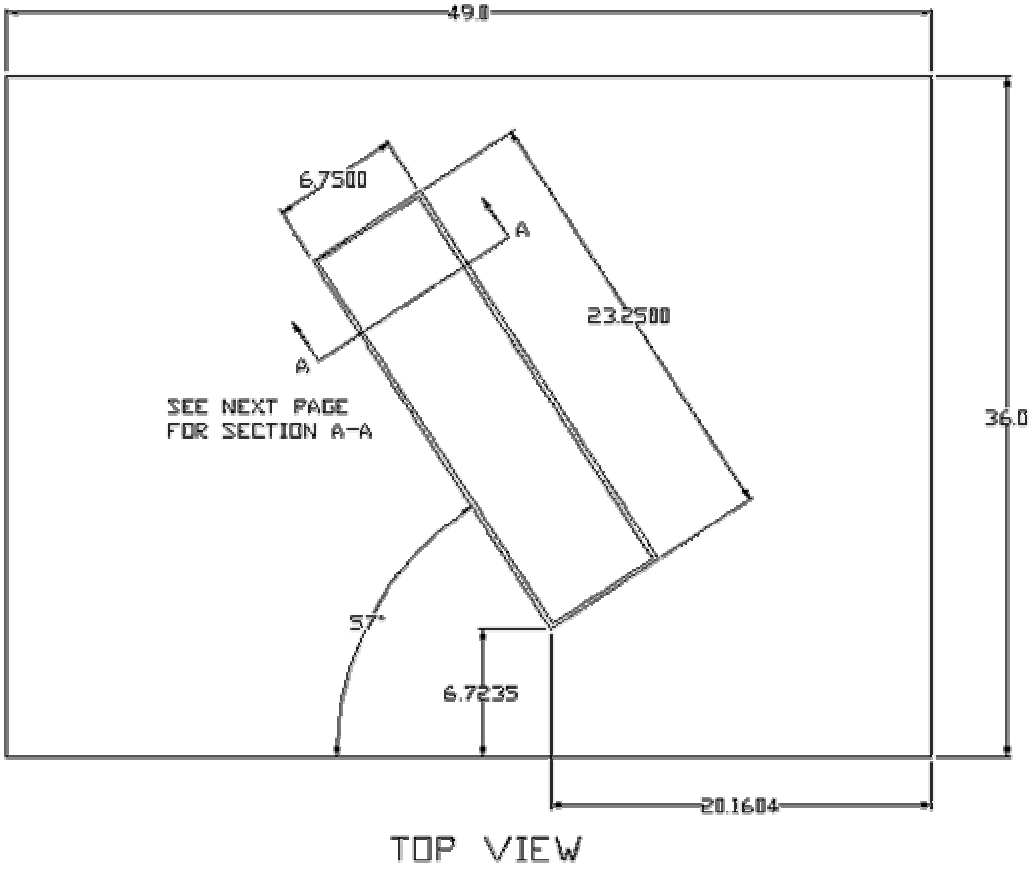

Figure E-1 Top view of the lexan shroud with machined slot for window and lid.

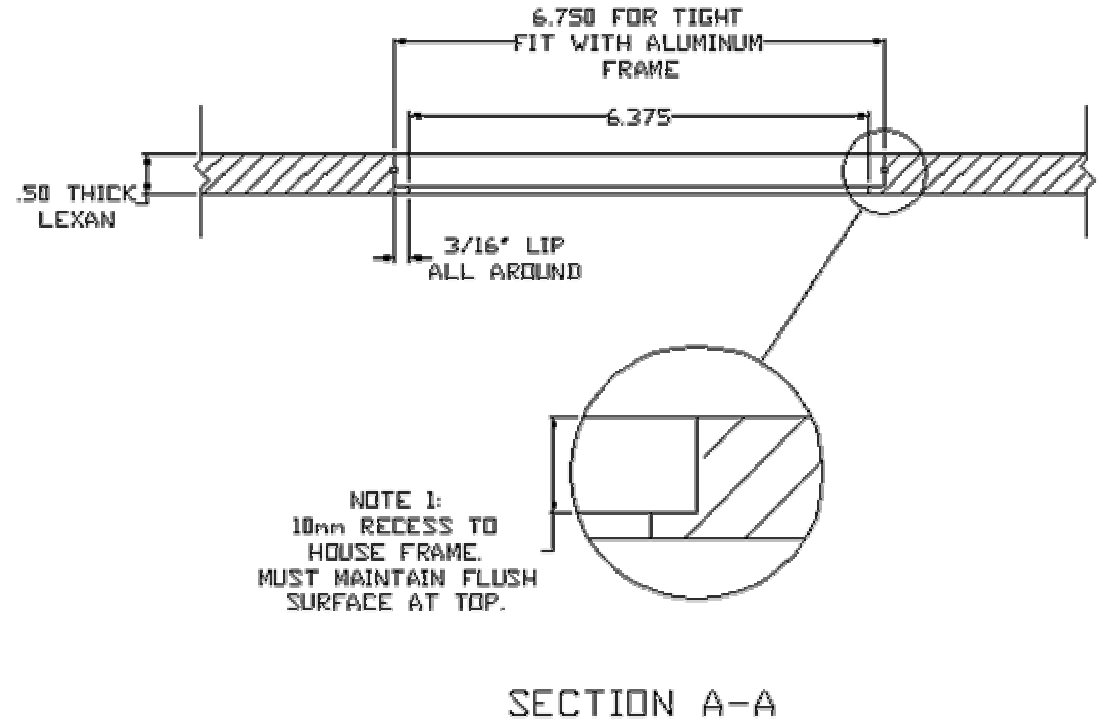

Figure E-2 Section view of the lexan shroud.

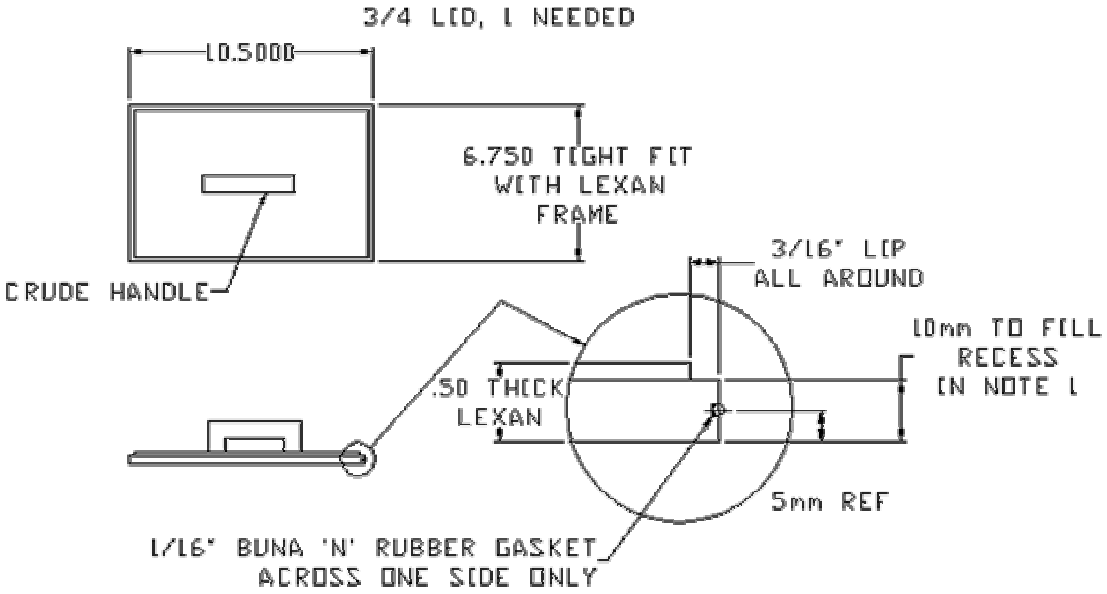

Figure E-3 Lexan filler lid to seal space not occupied by the IR window and frame.

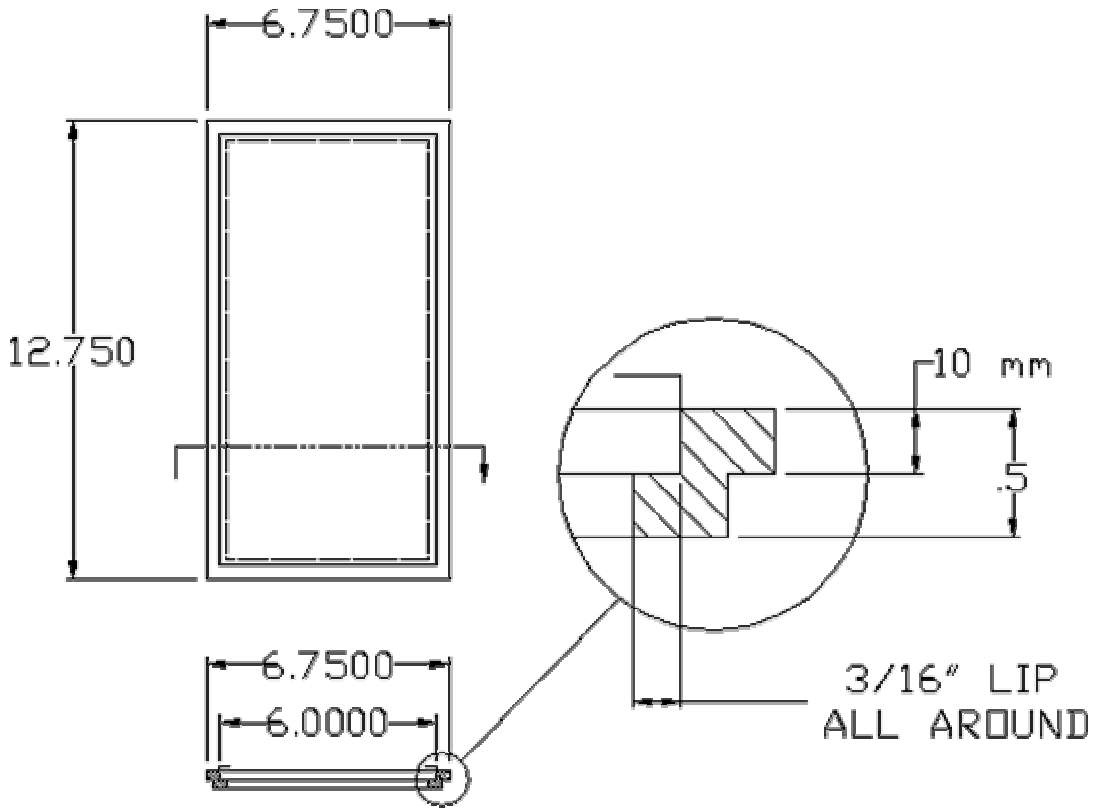

Figure E-4 Aluminum frame for housing two 10 mm thick, 6 in x 6 in ZnSe windows.

Appendix F. Calculations for Uncertainty Analysis

This appendix presents the uncertainty analysis calculations.

Effectiveness Measurements, η and ϕ

$$\boxed{\eta, \phi = \frac{T_\infty - T}{T_\infty - T_c}}$$ where $T = T_{aw}$ for η values and $T = T_m$ for ϕ values.

$$U_{\eta,\phi} = \sqrt{\left(\frac{\partial(\eta,\phi)}{\partial T}\cdot u_T\right)^2 + \left(\frac{\partial(\eta,\phi)}{\partial T_\infty}\cdot u_{T_\infty}\right)^2 + \left(\frac{\partial(\eta,\phi)}{\partial T_c}\cdot u_{T_c}\right)^2}$$

$$\frac{\partial(\eta,\phi)}{\partial T} = \frac{1}{T_\infty - T_c}$$

$$\frac{\partial(\eta,\phi)}{\partial T_\infty} = \frac{T - T_\infty}{(T_\infty - T_c)^2} + \frac{1}{T_\infty - T_c}$$

$$\frac{\partial(\eta,\phi)}{\partial T_c} = \frac{T_\infty - T}{(T_\infty - T_c)^2}$$

High Value of $\eta, \phi = 1.00$

Variable	Value	Precision Uncertainty (°C)	Bias Uncertainty (°C)	Total Uncertainty
η, ϕ	1.00	–	–	0.026 (2.6%)
T	27.91	0.313	0.45	0.55
T_∞	50.7	–	–	0.2
T_c	27.9	–	–	0.2

Low Value of $\eta, \phi = 0.20$

Variable	Value	Precision Uncertainty (°C)	Bias Uncertainty (°C)	Total Uncertainty
η, ϕ	0.2	–	–	0.025 (12.5%)
T	46.14	0.313	0.45	0.55
T_∞	50.7	–	–	0.2
T_c	27.9	–	–	0.2

Pressure Coefficient Measurements, C_p

$$C_p = \frac{P_{s,local} - P_{s,inlet}}{P_{dynamic}} = \frac{(P_a - P_{s,inlet}) - (P_a - P_{s,local})}{P_{dynamic}} = \frac{\Delta P_{s,inlet} - \Delta P_{s,local}}{P_{dynamic}}$$

$$U_{C_p} = \sqrt{\left(\frac{\partial C_p}{\partial \Delta P_{s,inlet}} \cdot u_{\Delta P_{s,inlet}}\right)^2 + \left(\frac{\partial C_p}{\partial \Delta P_{s,local}} \cdot u_{\Delta P_{s,local}}\right)^2 + \left(\frac{\partial C_p}{\partial P_{dynamic}} \cdot u_{P_{dynamic}}\right)^2}$$

$$\frac{\partial C_p}{\partial \Delta P_{s,inlet}} = \frac{1}{P_{dynamic}}$$

$$\frac{\partial C_p}{\partial \Delta P_{s,local}} = -\frac{1}{P_{dynamic}}$$

$$\frac{\partial C_p}{\partial P_{dynamic}} = \frac{\Delta P_{s,local} - \Delta P_{s,inlet}}{\left(P_{dynamic}\right)^2}$$

Uncertainties within 0-5 inH2O transducer range:

High Value of C_p = 17.3

Variable	Value	Precision Uncertainty (inH2O)	Bias Uncertainty (inH2O)	Total Uncertainty
C_p	17.3	–	–	1.29 (7.4%)
$\Delta P_{s,inlet}$	0.080	0.021	0.003	0.021
$\Delta P_{s,local}$	5.00	0.021	0.05	0.054
$P_{dynamic}$	0.285	0.021	0.003	0.021

Low Value of C_p = -17.8

Variable	Value	Precision Uncertainty (inH2O)	Bias Uncertainty (inH2O)	Total Uncertainty
C_p	-17.8	–	–	1.33 (7.5%)
$\Delta P_{s,inlet}$	0.080	0.021	0.003	0.021
$\Delta P_{s,local}$	-5.00	0.021	0.05	0.054
$P_{dynamic}$	0.285	0.021	0.003	0.021

Uncertainties above 5 inH2O measured by 0 – 20 inH2O manometer:

High Value of C_p =45.7

Variable	Value	Precision Uncertainty (inH2O)	Bias Uncertainty (inH2O)	Total Uncertainty
C_p	45.7	–	–	3.39 (7.4%)
$\Delta P_{s,inlet}$	0.080	0.021	0.003	0.021
$\Delta P_{s,local}$	13.1	–	–	0.1
$P_{dynamic}$	0.285	0.021	0.003	0.021

Low Value of C_p =-55.7

Variable	Value	Precision Uncertainty (inH2O)	Bias Uncertainty (inH2O)	Total Uncertainty
C_p	-55.7	–	–	4.18 (7.5%)
$\Delta P_{s,inlet}$	0.093	0.021	0.003	0.021
$\Delta P_{s,local}$	-16	–	–	0.1
$P_{dynamic}$	0.285	0.021	0.003	0.021

Appendix G. Tip h_{gc} Contours.

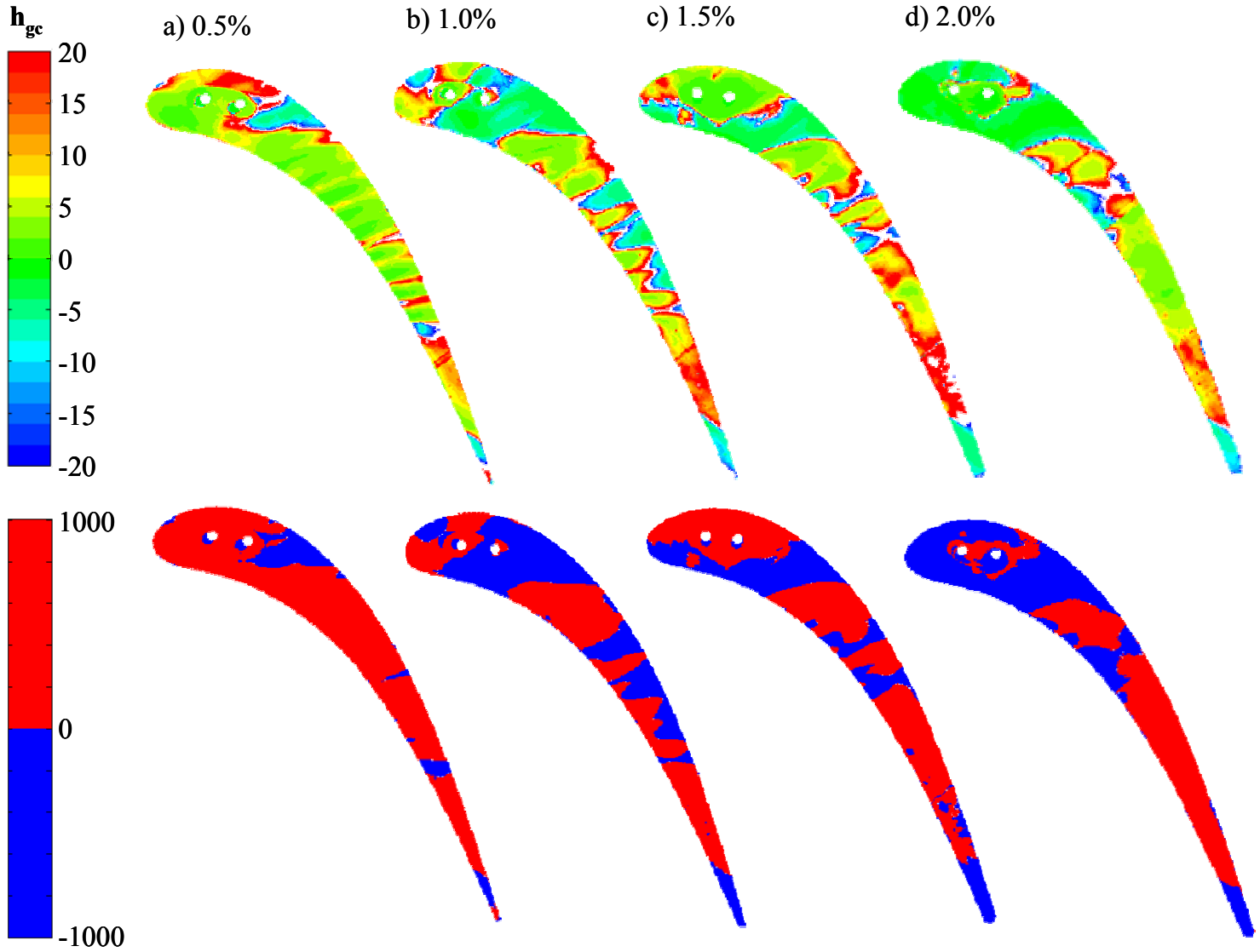

Figure G-1 Heat transfer coefficient ratio contours for a large tip gap.

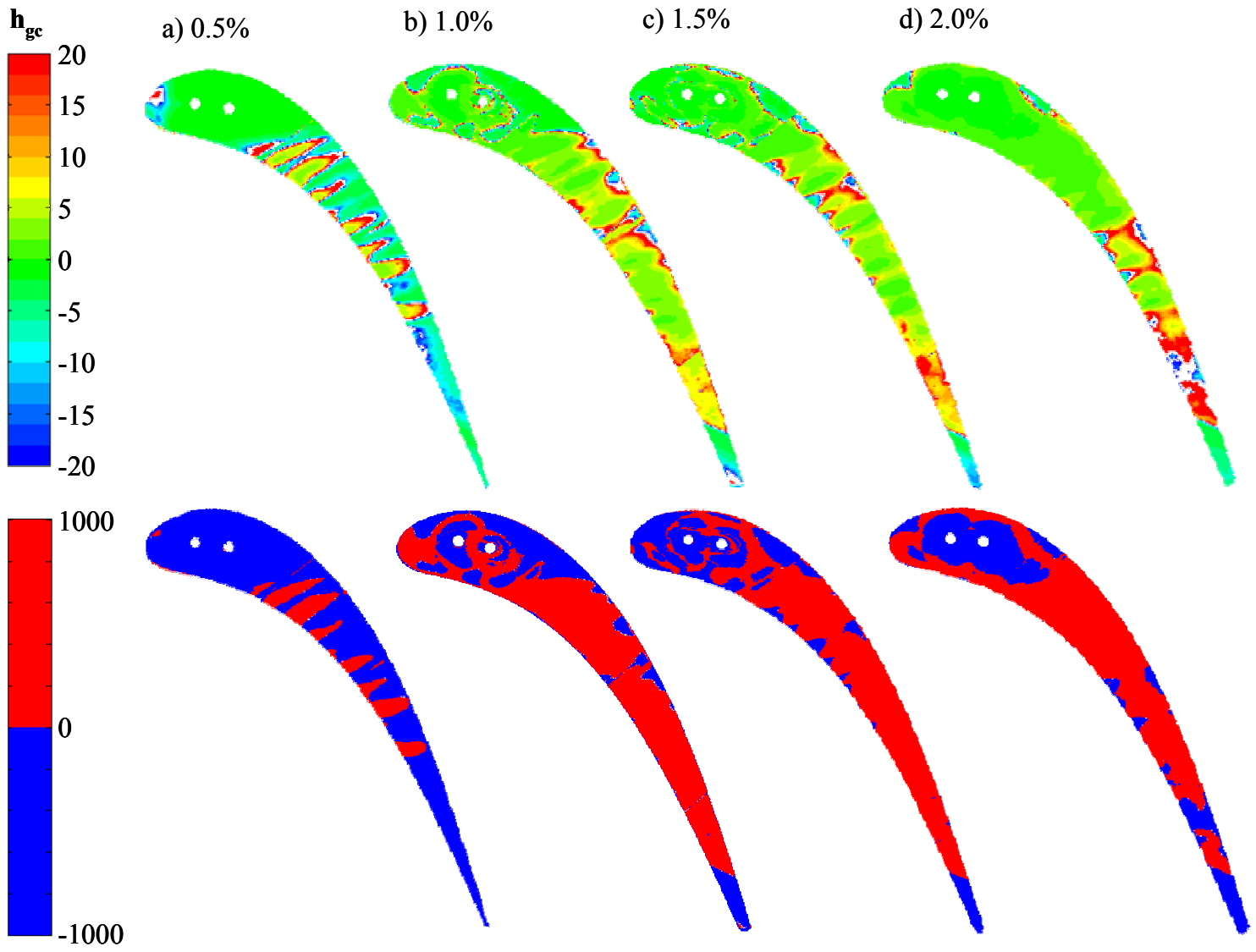

Figure G-2 Heat transfer coefficient ratio contours for a small tip gap.